Article

The Contribution of the Hulene-B Waste Dump (Maputo, Mozambique) to the Contamination of Rhizosphere Soils, Edible Plants, Stream Waters, and Groundwaters

Bernardino Bernardo [1,2]**, Carla Candeias** [1,]*** and Fernando Rocha** [1]

[1] GeoBioTec Research Centre, Department of Geosciences, University of Aveiro, 3810-193 Aveiro, Portugal
[2] Faculty of Earth Sciences and Environment, Pedagogical University of Maputo, Maputo 2482, Mozambique
* Correspondence: candeias@ua.pt

Abstract: The contamination of ecosystems in areas around waste dumps is a major threat to the health of surrounding populations. The aim of this study is to understand the contribution of the Hulene-B waste dump (Maputo, Mozambique) to the contamination of edible plants, rhizosphere soils, stream waters, and groundwater, and to assess human health risk. Soil and plant samples were analyzed by XRD and XRF for mineralogical and chemical composition characterization, respectively. Mineral phases identified in rhizosphere soil samples were ranked, calcite ($CaCO_3$) > quartz (SiO_2) > phyllosilicates (micas and kaolinite) > anhydrite ($CaSO_4$) > K feldspar ($KAlSi_3O_8$) > opal ($SiO_2 \cdot nH_2O$) > gypsum ($CaSO_4 \cdot 2H_2O$), suggesting potential toxic elements low mobility. Soil environmental indices showed pollution by Pb > Cu > Zn > Zr. The chemical composition of edible plants revealed contamination by Ni, Cr, Mn, Fe, Ti, and Zr. Groundwaters and stream waters showed a potential health risk by Hg and, in one irrigation water sample, by Pb content. The health hazard index of rhizosphere soils was higher by ingestion, with children being the ones more exposed. Results suggested a combined health risk by exposure to edible plants, rhizosphere soils, stream waters, and groundwaters.

Keywords: edible plants; rhizosphere soil; water; risk assessment; Maputo

1. Introduction

Unplanned city development in developing countries together with demographic growth increases solid urban wastes production, often deposited in abandoned areas, compromising the environment and health of surrounding populations [1]. Groundwater is an important source of potable water, representing ~30% of the world's resource for drinking and domestics purposes [2], and stream water is an important source for irrigation purposes [3]. Stream waters and groundwaters in areas surrounding waste dumps are vulnerable to contamination [4]. Waste dumps are a source of leachates, as a result of deposited solid waste decomposition, compromising surrounding waters and soils. Hussein et al. [5] reported Hg, Cd, Pb, Mg, As, Zn, and Cu groundwater enrichment in landfills in Malaysia, posing a risk to human health. Parvin et al. [6] suggested that Pb-contaminated water consumption can result in a range of hematological, neurological, renal, gene mutation, central nervous system, and reproductive impairment outcomes. Chronic exposure to water with high Zn content can induce stomach cramps, nausea, vomiting, anemia, and damage to the pancreas [7]. Other health hazards reported in the surroundings of waste dumps were linked to contaminated agricultural products [8].

Romero et al. [9] showed that agricultural areas surrounding waste dumps were influenced by contaminants transported by the wind [10]. High concentrations of heavy metals in rhizosphere soils were identified as a potential health risk by inhalation, ingestion, and dermal contact, with farmers being the ones more exposed [11]. Additionally, the contamination of rhizosphere soils, i.e., soil immediately surrounding the plant root, can be

transported to edible plants, through transfer mechanisms of absorbed potentially toxic elements (PTEs) [12]. Sharma et al. [13] suggested that food crops from contaminated sites can represent a hazard at the trophic level in the food chain, with increased bioaccumulation of different elements. Contaminated plants can trigger several diseases in consumers, depending on PTEs content and their bioaccessibility [14]. Zhou et al. [15] suggested that pregnant women and children that consumed contaminated plants (e.g., Pb, Cd, Cu, Zn, and As) were at greater risk.

In Mozambique, among the causes of urban ecosystems contamination are waste dumps [16], with Maputo, the capital, having the largest areas of uncontrolled solid waste disposal [17]. The production of municipal solid waste increased rapidly, with a daily waste deposition in the Hulene-B dump of ~1000 t [18]. All types of domestic, urban, clinical/hospital, and industrial wastes are deposited without previous treatment or control [19]. Cendón et al. [20] and Nogueira et al. [21] reported that the Maputo aquifer system is vulnerable to contamination given the shallow groundwater depth. Bernardo et al. [22], reported a possible migration of leachates causing contamination of surrounding soils, stream waters, and groundwaters. Vicente et al. [23], and Bernardo et al. [24] suggested enrichment of soils and groundwater by Cr, Cu, Mn, Pb, Zn, and Zr in the vicinity of the Hulene-B dump. Studies on the contamination of edible plants, cultivated around dump studies, are scarce, although the practice of horticulture is common in local houses backyards. The aim of this study is to understand the contribution of the Hulene-B waste dump to the contamination of stream waters, groundwaters, edible plants, and rhizosphere soils and to assess risk to human health. Results can contribute to understand the contamination mechanisms of the ecosystem around the dump, which can help local governments to take adequate measures to mitigate the impacts of the Hulene-B dump. The present study uses recent methods and an integrated approach to the systemic study of environmental impact and health risk posed by waste dumps on the surrounding population.

2. Methods and Materials

2.1. Study Area

Hulene-B waste dump (Figure 1) is located in the northern area of Maputo (Mozambique) and occupies an area of ~17 hectares [18]. Around the dump are located Hulene-B and Laulane neighborhoods, with 48,717 and 27,061 inhabitants, respectively [25]. Matsinhe et al. [26], Sarmento [27], and Serra [18] reported that the dump receives all type of wastes produced in the city, e.g., industrial, domestic, commercial, and hospital, with an estimated ~1000 t/d being continuously compressed. The dump is located in an abandoned open-air quarry, and the first waste deposit dated from 1973 [28], having a waste height of ~6 to 15 m [29]. The dump is positioned on a dune slope with E–W orientation, with stream water and leachates migrating in the same direction, mostly during rainy season [17]. The dump's W area was improved in 2018, after a large waste mass collapse that buried several houses and caused the death of 17 inhabitants [30]. The improvement works consisted on the removal of all houses near the dumpsite, creating an empty area. From 2020, this area began to be occupied by crop fields around the riparian area, which accumulates surface water, including dispersed leachates from the dumpsite and runoff water from Julius Nyerere Avenue (Figure 1). This wetland surrounding Hulene-B, is used for the practice of subsistence agriculture, predominantly cabbage, lettuce, sweet potato, and pumpkin [16].
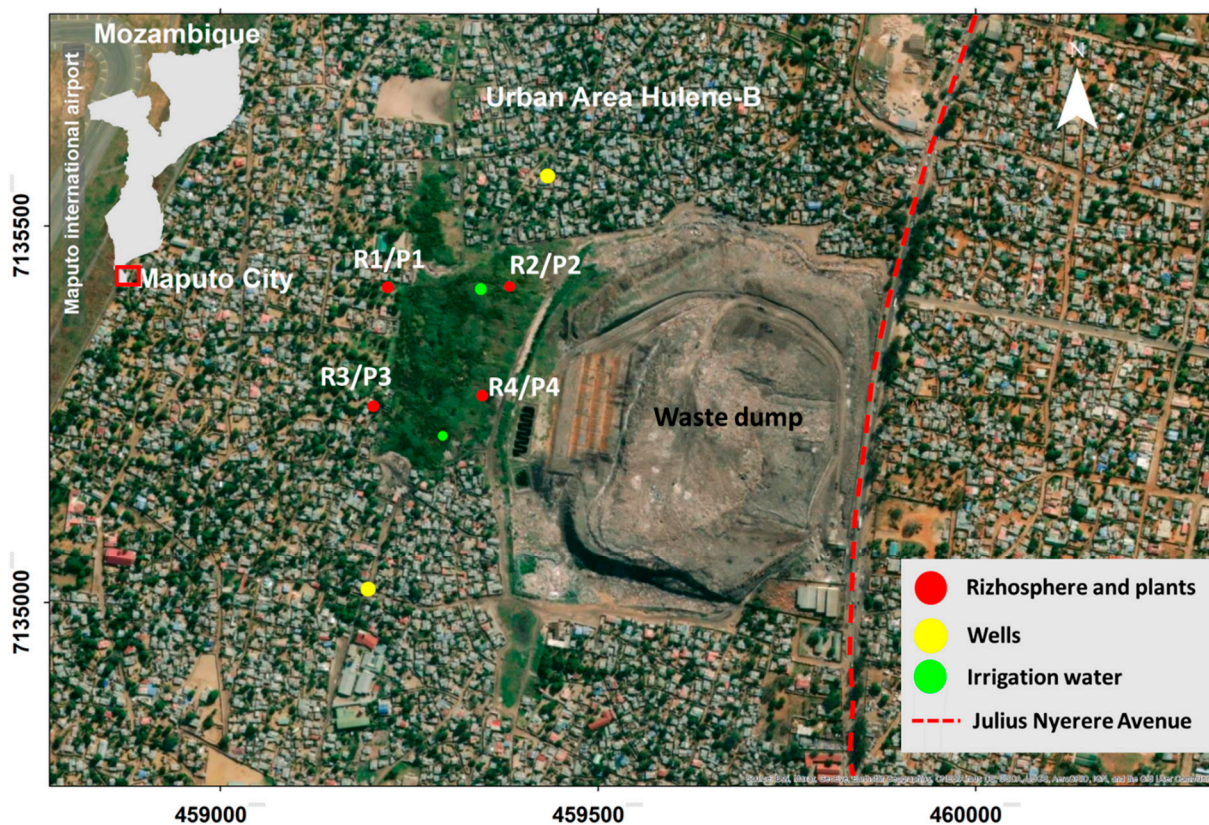
Figure 1. Sampling locations, and surrounding environment, with numerous dwellings surrounding Hulene-B waste dump (center), airport (NW), and Julius Nyerere Avenue (E).

Hulene-B hydrogeological system is part of the Tertiary to Quaternary aquifer system [20], with a substrate of clayey marl to grey clay layers [20,21]. In the western limit of Hulene-B dump, there is a semi-impermeable layer of clayey sands, fine-to-coarse sand, and sandstones, facilitating water circulation between these two sectors [21]. Well water levels, in the surroundings of the waste dump, varies between 1.5 and 9.3 m in deep [20]. Until 1990s, population use of groundwater was common in the surrounding of the dump; however, many wells were decommissioned in recent years due to high levels of groundwater contamination [31]. Soils on the western border of the dump are mostly composed of materials from upper Pleistocene Malhazine Formation (QMa) and upper Pleistocene to lower Pleistocene Red Point Formation (TPv) [32]. The Malhazine Formation, on the western border, consists of coarse-to-fine, poorly consolidated sands with whitish to reddish colors, fixed by vegetation and consolidation processes. The predominant climate is subtropical, with two seasons: (a) hot and rainy period from December to March, with >60% of annual precipitation, with intense precipitation in January (average 125 mm); (b) dry and cold season from April to September, with lower temperatures in June and July, and weak and irregular precipitation with minimum intensity in August (~12 mm). The average annual precipitation is ~789 mm, and prevailing SE winds [33].

2.2. Rhizosphere Sampling and Analysis

Four rhizosphere composite soils samples (R1 to R4; ~1.5 kg each) were collected on agricultural areas on the W of the dump (Figure 1). Samples were georeferenced and preserved in clean plastic bags until laboratory treatment. In the laboratory, samples were dried in an oven ≤40 °C, homogenized, and sieved (<2 mm), at Pedagogical University of Maputo, Mozambique. Afterwards, samples were transported to GeoBioTec research center laboratories (University of Aveiro, Portugal, UAVR), for physical, chemical, and mineralogical analyses. Electrical conductivity (EC) and pH were determined in a 1:2.5 soil/water

solution using a high-resolution pH meter and condutivimeter. Organic matter (OM) content was determined by the method described by USDA [34]. Color was determined according to [35]. Soil pH was classified according to USDA [36] as extremely acidic 3.5–4.4, very strongly acidic 4.5–5.0, strongly acidic 5.1–5.5, moderately acidic 5.6–6.0, slightly acidic 6.1–6.5, neutral 6.6–7.3, slightly alkaline 7.4–7.8, moderately alkaline 7.9–8.4, and strongly alkaline 8.5–9.0. Soil organic matter was classified as: high content > 4%, medium content 2–4%, and low content < 2% [34]. Electrical conductivity was classified taking in consideration reference values for soil salinity for horticultural crops ($\leq$1100 µS/cm) and for sandy soils EC (<100 µS/cm) [37]. Chemical composition was accessed by X-ray Fluorescence (XRF), using a PANalytical PW 4400/40 45 Axios (Malvern Panalytical, Almelo, The Netherlands) with Cr Kα radiation. Mineralogy was determined by powder X-ray Diffraction (XRD), using a Phillips/Panalytical powder diffractometer (Malvern Panalytical, Almelo, The Netherlands), model X'Pert-Pro MPD, equipped with an automatic slit. A Cu-X-ray tube was operated at 50 Kv and 30 mA. Data were collected from 2 to 70° 2θ with a step size of 1° and a counting interval of 0.02 s. Results were within the 95% confidence limit, with precision and accuracy of analyses and digestion procedures monitored by internal standards, certified reference material, and quality control blanks. Relative Standard Deviation was between 5% and 10%.

2.3. Edible Plants Sampling and Analysis

Four cultivated edible plants (Figure 2a–c) were collected at the same rhizosphere soil locations (Figure 1). The species collected were sample RP1: Amaranthus leaves (*Amaranthus spinosus*), at the western end of the riparian zone; sample RP2: sweet potato leaves (*Ipomoea batatas*), at the eastern end of the riparian zone; sample RP3: cabbage leaves (*Brassica oleracea L*), at south-western end of the dump; and sample RP4: pumpkin leaves (*Cucurbita pepo*), at the south-eastern end. Plant leaves are consumed by the inhabitants, having been planted near the riparian zone due to soil humidity and proximity of stream water used for irrigation. After plants collection (~400 g of fresh leaves), samples were transported to the laboratory and dried in an oven at ~40 °C. Chemical analyses of the plants were performed by XRF, at GeoBioTec (UAVR) laboratories.
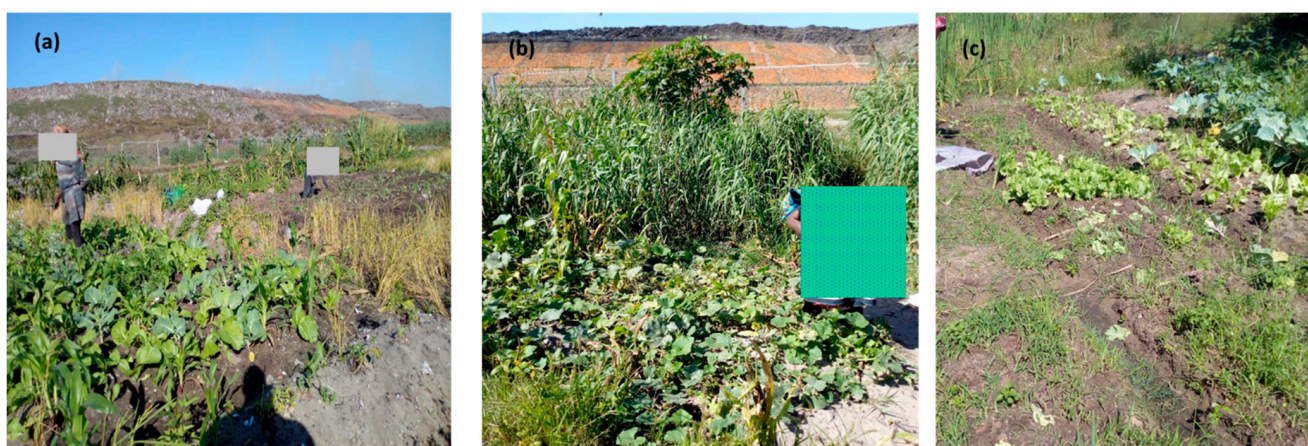
Figure 2. Edible plants cultivation near Hulene-B waste dump.

2.4. Water Sampling and Analysis

Four representative water samples were collected (Figure 1): 2 stream water samples used for irrigation, in north-western (IWN) and south (IWS) areas; and 2 groundwater samples from wells used for human consumption, located south-west (WS) and north-west (WN) of the dump. Sample WS was collected at 5 m depth, on an uncovered well, and sample WN, was collected at 8 m depth on a covered well. Each sample was collected and preserved (4 °C) in clean 1 L polyethylene bottles and transported to the laboratory for

analysis. Waters pH was measured in situ, being classified as acidic < 7, neutral = 7, or basic > 7 [38]. Water samples chemical analysis was performed using a Metalyser H1000 (Trace2o, Berkshire, United Kingdom) Trace-2 to analyze Pb, Hg, Zn concentrations. This equipment is recommended in the analysis of heavy metals given its robustness, accuracy and a 97% correlation with Atomic Absorption Spectrometry (GF-AAS) analysis [39].

2.5. Soil Indexes and Health Risk Assessment (SHRA)

Soil pollution index (PI) was calculated for PTEs Cr, Cu, Fe, Mn, Ni, Pb, Ti, Zn, and Zr, by dividing the individual mean concentration (C_i) by their corresponding reference values for rhizosphere soils (Cd) − PI = C_i/C_d. Pollution index classifies soils as slightly polluted ($0 \leq PI < 1$), moderately polluted ($1 \leq PI < 3$), highly polluted ($3 \leq PI < 6$), and very highly polluted ($PI \geq 6$) [40].

Pollution Load index (PLI) provides a simple comparative mean to assess soils level of PTEs contamination, by the same PTEs, as the nth root of the product of the nPI, with n being the number of variables (PTEs) considered: PLI = $(PI_1 \times PI_2 \times PI_3 \times \cdots \times PI_n)^{1/n}$. When PLI > 1, environmental deterioration must be considered [41].

Soil health risk assessment (SHRA) was calculated taking in consideration inhabitants' exposure, for both children and adults, through ingestion, inhalation, and dermal contact [42]. Parameters considered were: ingestion rate of 200 and 100 mg/d for children and adults, respectively; inhalation rate of 7.6 and 20 m^3/d for children and adults, respectively; exposure frequency of 180 d/year; exposure period (EP) of 15 years for non-carcinogenic effects in children and adults, respectively; 60 years as a lifetime (LT) for carcinogenic effects; mean body weight of 15 and 60 kg for children and adults, respectively; mean time to non-carcinogenic effects = EP × 365 days; exposed skin area of 2800 and 5700 cm^2 for children and adults, respectively, and skin adhesion factor of 0.2 and 0.07 mg/cm^2 for children and adults, respectively; dermal absorption factor of 0.001 for selected PTE (Cr, Cu, Fe, Mn, Ni, Pb, Ti, Zn, and Zr), and age-adjusted dermal soil contact factor of 362 mg·yr/kg·d; mean time to carcinogenic effects = LT × 365 days; and exposure time of 8 h/d [43]. Carcinogenic and non-carcinogenic side effects for each element were computed individually, considering reference toxicity levels for each variable, as extensively described [42,44]. For each selected PTE and pathway, non-cancer toxic hazard was estimated by computing the Hazard Quotient (HQ) for systemic toxicity (i.e., non-carcinogenic risk). If HQ > 1, non-carcinogenic effects might occur as the exposure concentration exceeds the reference dose (RfD). The cumulative non-carcinogenic hazard index (HI) corresponded to the sum of HQ for each pathway and/or variable. Similarly, HI > 1 indicates that non-carcinogenic effects might occur. Carcinogenic risk, or the probability of an individual to develop any type of cancer over a lifetime because of exposure to a potential carcinogen, was estimated by the sum of total cancer risk for the three exposure routes. A risk > 1.00×10^{-6} is the carcinogenic target, while values > 1.00×10^{-4} are considered unacceptable [43].

2.6. Soil/Plant Transfer Factor (TF)

Transfer factor allowed us to assess transfer of elements from soils to edible plants and was calculated as follows: TF = C_{plant}/C_{soil}, where C_{plant} and C_{soil} are the individual element concentration (mg/kg) in edible plants and soils samples, respectively. TF > 1 indicates an accumulation of elements [44].

2.7. Plant Health Risk Assessment (PHRA)

Plant health risk assessment (PHRA) is used to evaluate human health risk associated with the consumption of contaminated plants [45]. Was estimated through the daily elemental intake (DIM), the hazard risk index (HRI), the targeted hazard quotient (THQ), and the hazard index (HI_{plant}). Plants DIM by adults does not consider body's metabolic response to PTEs; however, it may indicate a possible rate of intake of a selected PTE, with DIM = $C_{element} \times D_{intake}/B_{weight}$, where DIM is the daily adult elemental ingestion (kg/day), $C_{element}$ is the plant dry weight elemental concentration (mg/kg), D_{intake} is the

daily consumption of edible plants (*Amaranthus* leaves = sweet potato leaves = pumpkin leaves = cabbage = 0.025 kg/day), and B_{weight} is the average body weight (60 kg/adult) [45]. HRI by ingestion of edible plants for each element was calculated by HRI = DIM/RfD, where RfD is the reference oral dose (Cr = 0.003; Cu = 0.037; Fe = 18; Mn = 0.14; Ni = 0.2; Pb = 0.014; Ti = 0.7; Zn = 0.3; and Zr = 4.2 kg/day) [46]. Targeted hazard quotient was the ratio between PTEs dose and a reference dose (dimensionless) indicating the non-carcinogenic hazard through edible plants ingestion. It was calculated by THQ = (EF $\times$ ED $\times$ D_{intake} $\times$ $C_{element}$)/(RfD $\times$ B_{weigh}t $\times$ AT), where EF is the exposure frequency (300 days/year), ED is the exposure duration (40 years), and AT is the average exposure time (ED $\times$ 365 days/year). Hazard index (HI_{plant}) is the summation of all PTEs considered and given by HI = $\sum_{n=1}^{i}$ THQn, i = n, . . . n [47]. HRI, THQ, and HI values <1.0 indicate no risk by plant consumption, and if $\geq$1.0 adverse health effects should be considered [45].

2.8. Water Pollution Index (WPI)

The water pollution index was determined based on the measured concentrations of Hg, Pb, and Zn. Single factor pollution index was calculated as: $P_i = C_i/S_i$ [48], where P_i is the pollution index of pollution indicator i, C_i is the concentration of pollution indicator in water (mg/L), and S_i is the permissible limit for the pollution indicator in water, with P_i classified as: <0.4, non-pollution; 0.4–1.0, slightly polluted; 1.0–2.0, moderately polluted; 2.0–5.0, heavily polluted; and >5.0, seriously polluted [49].

2.9. Water Health Risk Assessment (WHRA)

Water health risk assessment was determined for Zn, Hg and Pb content [50,51]. Exposure was determined with reference values established by WHO [38,52], of Hg 2, Zn 3.000, and Pb 1 μg/L. Adjustable parameters used were daily water consumption of 1.5 and 2 L/day for children and adults, respectively; exposure frequency number of days exposed in a year of 365; total years of exposure of 15 and 60 for children and adults, respectively; average exposure time 5475 and 21,900 for children and adults, respectively; dermal permeability coefficient of 0.001 for all PTEs; surface area exposed of 852.5 and 1610 cm^2 for children and adults, respectively; skin adherence factor of 0.2 and 0.07 for children and adults, respectively. Carcinogenic risk and non-carcinogenic hazard were determined using similar methods used for SHRA [53].

3. Results and Discussion

3.1. Soil Analysis

Rhizosphere soils pH, electrical conductivity (EC), organic matter (OM), and color are presented in Table 1. Soil pH is an important property which controls chemical reactions of metals [47]. Rhizosphere soils revealed a moderately alkaline pH (8.1–8.4), confirming the findings of Naveen et al. [54] that, in general, areas impacted by heavy metals from dumps tend to have higher pH. Gajaje et al. [55], in their study on soils around Morupule dumpsite (Botswana), found an average pH of 8.3 in rhizosphere soils and associated it with heavy metal contamination (Cu, Cr, Mn, and Pb). Skrbic et al. [56], suggested that the PTEs highest retention in rhizosphere soils occurred with high pH, due to lower metals solubility in this pH range. Alkaline pH might affect plant growth because of the difficulty in absorbing essential plant nutrients, as well as PTEs, e.g., Fe, Mn, Cu, and Zn [36].

**Table 1.** Rhizosphere soils pH, electrical conductivity (EC; in µS/cm), organic matter (OM; in %), and color.

ID	pH	EC	OM	Color
R1	8.1	510	3.6	blackish
R2	8.4	571	1.7	greyish
R3	8.2	310	0.98	greyish
R4	8.4	810	2.3	greyish

EC showed high values, when compared to sandy soils guidelines ($\leq$100 µS/cm; Lund, 2008), being ranked R4 >> R2 > R1 > R3. Bhardwaj et al. [39] suggested that rhizosphere soils in areas near waste dumps, usually exhibit higher EC values, being associated with contamination by metal ion enriched leachates [5], and deposition of contaminated ashes resulting from waste incineration [57]. Bernardo et al. [24], reported high EC values and high Cr, Cu, Mn, Ni, Pb, Zn, and Zr concentrations in the Hulene-B dump surrounding soils, associating it with leachates. Another factor that may be associated with high EC is the presence of shallow water [58]. In sandy soils, the presence of water during rainfall episodes and periodic enrichment by surface leachates promote EC [37]. Studies related EC to crop yields and found that high EC values can reduce yields [59]. However, for horticultural crops, EC (salinity) results were considered within the recommended limit (<1000 µS/cm) [60].

Soil OM content was ranked R1 > R4 > R2 > R3, coherent with other studies, with generally low OM [61]. Some studies have shown that in contaminated areas, high OM content in rhizosphere can lead to the uptake of heavy metals, which bind easily to OM [34] and consequently decrease their toxicity levels from the rhizosphere to crops [62]. Rhizosphere soils color was classified as very dark in all samples, with sample R1 the darkest, associated with its OM content, which can be incorporated in interstitial spaces of sandy soils [63]. Bernardo et al. [64] linked the Hulene-B surrounding soils color variation to leachates circulating freely on the soil surface and waste incineration ashes, which can be associated with rhizosphere soils PTEs contamination [65], which can be transferred to edible plants [66].

Mineral phases are identified on the studied rhizosphere soils, where quartz (SiO_2), calcite ($CaCO_3$), phyllosilicates (micas and kaolinite), anhydrite ($CaSO_4$), K feldspar ($KAlSi_3O_8$), opal ($SiO_2 \cdot nH_2O$), and gypsum ($CaSO_4 \cdot 2H_2O$) can be found (Figure 3), thus suggesting differentiated processes between intra-dune and other soils around the Hulene-B dump. Quartz content (18.1 to 40.5%) was similar to intra-dune deposits [32], which also revealed high calcite content. Samples R2 and R4 showed a higher calcite content, possibly due to the influence of soils remobilization in depth during the construction of the leachate transport channels.

Phyllosilicates content (3.0 to 28.8%) may be linked to the predominant aeolian and superficial deposition processes of the intra-dune area. Previous studies suggested that phyllosilicates content present a higher PTEs adsorption capacity, e.g., [67]. Quartz, under conditions of exceptional morphology fracture, can adsorb PTEs, such as Pb, Cu, and Cr [68]. Calcite has been reported to have the ability to immobilize heavy metals such as Pb, Fe, and Cd in contaminated soils near areas such as dumpsites [69].
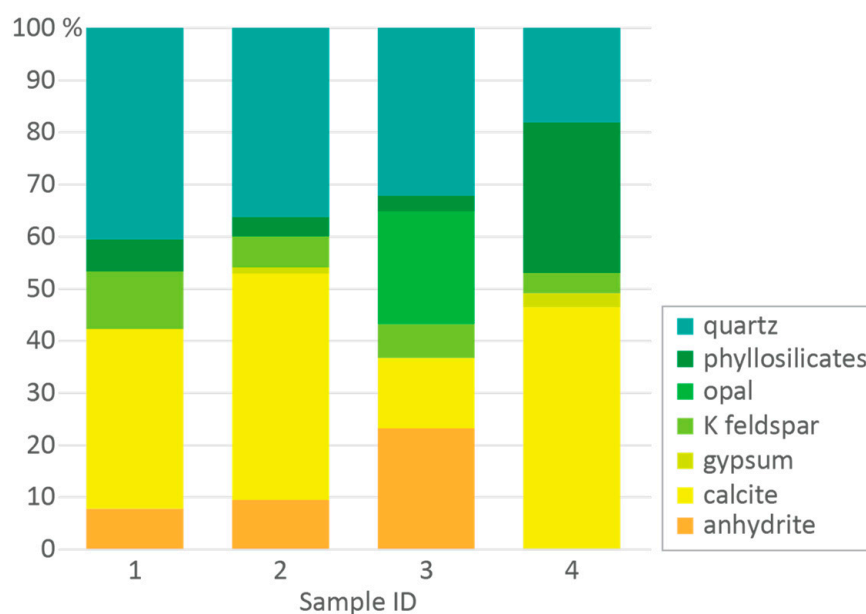
Figure 3. Mineral phases identified on rhizosphere soils (relative quantification, in %).

Soils PTEs (Table 2) revealed significant differences (one sample *t*-test; $p < 0.05$) between samples Cr, Fe, Mn, Ti, and Zr content. The cluster analysis formed two major groups, one with sample R1 and another with samples R2 and R4, revealing an association to mean background values, and these three variables were grouped with sample R3. Sample R1 presented higher PTEs concentrations than other samples. The results suggested an external Cu, Ni, Pb, Ti, Zn, and Zr contamination contribution, especially in sample R1. This sample was collected on northwest section of the dump, relatively distant, suggesting contamination by transported waste incineration ash, with this location being in the direction of displacement and deposition of windborne suspended materials.

Table 2. Rhizosphere soil samples and potentially toxic elements content of background soils (Bkg) (in mg/kg).

Var	R1	R2	R3	R4	Bkg *
Cr	18.5	13.0	6.8	8.9	33.5
Cu	184	88	24	351	9.2
Fe	15,966	5954	3195	5480	6801
Mn	153	120	93	113	140
Ni	14.6	4.2	2.6	4.9	3.9
Pb	156	39.0	9.7	156	7.8
Ti	2782	2116	1775	1703	1754
Zn	35.7	38.7	3.7	9.8	3.0
Zr	289	207	170	148	123

* Bernardo et al. [70]

The rhizosphere soil pollution index (PI) of sample R1 revealed low pollution considering Cr, moderate pollution by Zr, Fe, and Ti, and high to very high pollution by Cu, Pb, Zn, and Ni (Table 3). Sample R2 Cu, Pb, and Zn content contributed to a very high PI; Ni, Ti, and Zr contributed to a moderate PI; and Ti contributed to a high PI. Similar results were found for samples R3 and R4. The higher contributions of Cu, Pb, Zn and Ni PI values in sample R1 may be associated with location, i.e., near the waste incineration and Julius Nyerere Avenue on the W, with sources of ash and contaminated dust. High concentrations of Cu, Pb, Zn, and Ni were reported in road dust samples next to the Hulene-B dump, being associated with waste incineration, intense traffic, and pavement degradation [70]. Samples R2 and R4 showed higher Cu, Pb, Zn, Ni, Ti, and Zr content, possibly linked to

the superficial circulation of leachates, which occurs cyclically. Bernardo et al. [70] reported high EC values and associated a possible contamination by leachate flows. Sample R3 presented a high PI with respect Cu, associated with surface water enriched by leachates circulation.

Table 3. Pollution index and pollution load index of the studied rhizosphere soil samples.

Var	PI				PLI
	R1	R2	R3	R4	
Cr	0.6	0.4	0.0	0.3	0.0
Cu	20.0	9.6	2.6	38.2	4748
Fe	2.4	0.9	0.5	0.8	0.2
Mn	1.1	0.9	0.7	0.8	0.1
Ni	3.7	1.1	0.7	1.3	0.8
Pb	20.0	5.0	1.2	20.0	618
Ti	1.6	1.2	1.0	1.0	0.5
Zn	11.9	7.2	0.4	3.3	26.4
Zr	2.4	1.7	1.4	1.2	1.6

Pollution load index (PLI) was ranked Cu >> Pb >> Zn > Zr > Ni > Ti > Fe > Mn > Cr, suggesting environmental deterioration in the surrounding area of the dumpsite. Sample R1 was the one that contributed most PTEs and had a high rate of contamination. Sample R1 was collected in the NW border of the dump, strongly influenced by waste incineration, with ashes regularly transported and deposited in this location. On the dump surroundings, the incineration of urban wastes, such as electronics, hospital waste, tires, and lamps, has been pointed out as a source of Cr, Cu, Mn, Ni, Pb, and Zn [57]. Sample R4 was the one that most contributed to this index, with high Cu and Pb content, and it was collected at the SW border of the dump, where surface dispersion of leachate predominates. Leachates have been identified as a source of PTEs in the surroundings of dumps [71] and are associated with higher OM content, which may influence the fixation of contaminants [72]. Sample R2, located north of the dump and close to the dump, with its relatively low contribution, may be associated with possible leaching of contaminants in this strip. However, the high pollution index by Cu, Pb, and Zn may be associated with the circulation of leachates that cyclically affect this area. However, sample R3 showed a low contribution, which may be related to its relatively distant location from the Hulene-B dump. High contributions of Cu may be associated with new deposits in the southwest, where open-air burning and ash deposition are recorded in the surrounding soils.

Rhizosphere soils hazard quotient (HQ) by ingestion and dermal contact for children was considered, due to higher risk by playing on the ground and hand-to-mouth behaviors in young age (Figure 4). All PTEs presented HQ > 1 by ingestion, except for Zr, with Mn being the element posing a higher hazard followed by Cu, Ti, and Zn. Dermal contact HQ was >1, except by Pb in samples R1 and R3, and Zr in all samples, with Ni and Mn being the PTEs posing a higher hazard. Prolonged exposure to Mn can induce pneumonia, hallucinations, pulmonary embolism, and bronchitis [71], while Ni poisoning affects lung function, breathing difficulties, coughing, skin or eye irritation, and chronic exposure to Cu can induce anemia and central nervous system and cardiovascular system disorders [73].
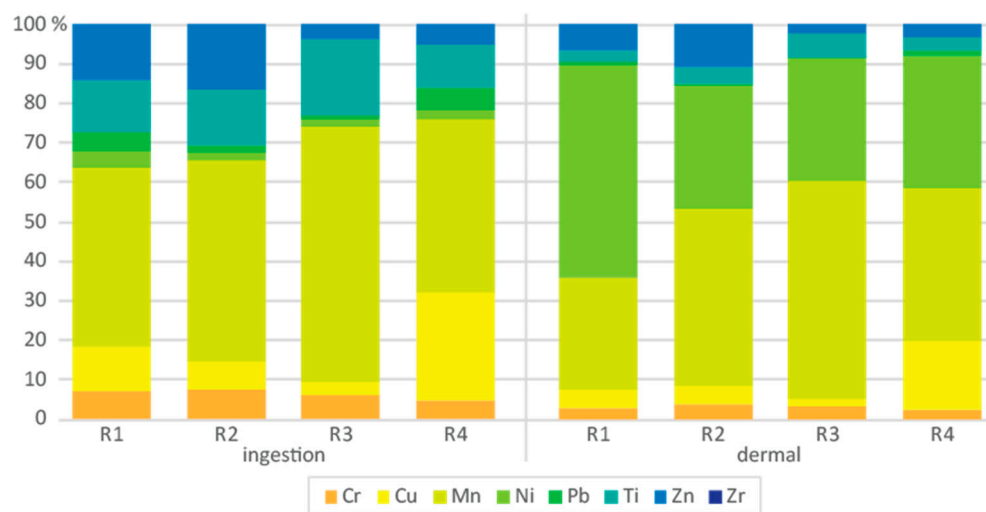
Figure 4. Rhizosphere soil hazard quotient (HQ) by ingestion and dermal contact for children (relative quantification, in %).

3.2. Water Analysis

Water pH was higher in stream waters, being higher than reference values (Table 4). Water sample WS presented a pH slightly below recommended for consumption [38]. pH is recognized to influence Hg, Pb, and Zn bioavailability and toxicity in drinking water [74]. Yesil et al. [75] reported higher bioavailability and toxicity of Hg and Pb in slightly acidic-to-neutral waters, such as sample WS, suggesting a greater health risk. Irrigation water IWN presented a higher Pb concentration than the reference value [52], which may be associated with ash deposition, as Pb contamination is caused by burning waste such as electronic equipment, batteries, paint cans, varnishes, and organic solvents, which is common [24]. In addition, free leachate circulation, which regularly reaches this area, is reported as a Pb dispersion source, in environments around waste dumps [6]. IWS showed high Hg content, which may also be associated with waste incineration [76].

Table 4. Water samples' pH, Pb, Hg, and Zn concentrations and reference values (in µg/L).

Var	Samples				Guidelines		
	WS	**WN**	**IWN**	**IWS**	**Drinking Water**	**Stream Water**	**Reference**
pH	6.1	8.4	9.1	10.3	6.5−8.50	5.5–7.5	WHO [53]
Pb	6	nd	79	nd	10	20	WHO [53]
Hg	36	76	nd	25	6	5	WHO [53]
Zn	63	13	7	9	3	≤5.000	WHO [53]; CCME [77]

nd—not detected.

The water pollution index revealed severe Hg P_i in the two water samples collected from wells (Table 5), while Pb P_i showed a slight pollution in sample WS and heavy P_i in IWN. Zinc P_i was classified as medium polluted in both wells and slightly polluted in IWS, taking in consideration Zn toxicity despite its higher concentration when compared to Pb and Hg content. Mercury can incorporate into groundwaters and surface waters through leachates produced at waste dumps by anaerobic decomposition of wastes or by particulate material resulting from the burning of contaminated wastes [76]. The practice of waste burning at the Hulene-B dump may be influencing the dispersion of ash enriched by heavy metals that were successively deposited in the vicinity of the waste dump and contributed to the contamination of groundwaters and stream waters. Lead enrichment in areas surrounding landfills has been associated with the deposition and burning of electronic equipment and rechargeable batteries wastes [78]. In the surroundings

of the Hulene-B dumpsite, other potential Pb sources may be linked to, e.g., traffic-related materials (Julius Nyerere Avenue) and an international airport (Figure 1). Zinc enrichment has been associated with batteries, alloys, paint cans, cosmetics, pharmaceuticals, textiles, and electrical and electronic equipment waste, which is continuously deposited and burnt in the Hulene-B dump [79].

Table 5. Pollution index (P_i) of groundwater and surface water.

ID	Pb	Hg	Zn
WS	0.6	6.0	2.1
WN	-	12.7	4.3
IWS	4.0	-	1.8
IWN	-	5.0	0.6

3.3. Edible Plants

The potentially toxic elements concentration in edible plants (Table 6) was higher than the daily reference dose (RfD) guidelines, suggesting a contribution from the Hulene-B dump. Studies suggested that waste dumps can be sources of PTEs on adjacent crops [80], with contamination also being associated with the transfer factor (TF) of contaminants from soil to plant [81]. Another mechanism of edible plants contamination in the vicinity of landfills is waste incineration ash deposition [82]. The consumption of these crops may represent a potential health risk [41]. The mean PTEs concentration of the edible plant samples was ranked RP1 > RP3 > RP2 > RP4. Sample RP1 (*Amaranthus spinosus*) was collected in the NW region of the dump, an area influenced by waste incineration ash deposition. However, Zr was not detected in edible leaves, despite its high concentrations in rhizosphere soils, suggesting a low TF under alkaline pH conditions [75]. Sample RP3 (*Brassica oleracea L*), collected relatively distant from the dump, showed high PTEs levels, despite rhizosphere soil contamination being relatively low, possibly associated with other contamination mechanisms such as cyclic, open-air incineration of waste occurring in a new area which may be a source of contaminated ash that accumulates on crop leaves. Sample RP2 (*Ipomoea batatas*) was collected relatively close to the dump, with PTEs content on rhizosphere soil being higher than the background mean, and plant edible leaves revealing a PTEs concentration above reference values. Yan et al. [12] suggested that *Ipomoea batatas* in contaminated soils presented higher capacity to absorb heavy metals such as Cu, Fe, Pb, and Zn. Sample RP4 (*Cucurbita pepo*) was collected at the S boundary of the landfill, and correspondent rhizosphere soil presenting higher PTEs concentration than local background. Plant edible leaves showed a higher content than RfD.

**Table 6.** Edible plants PTEs (in mg/kg).

Var	RP1	RP2	RP3	RP4	AL
Cr	974	852	2968	1161	2.3 [a]
Cu	1142	1245	778	1099	10–40 [a]
Fe	56,324	30,031	32,643	18,687	18 [a]
Mn	1030	1183	1436	1544	500 [a]
Ni	108	238	1128	538	10 [a]
Pb	394	56	190	nd	0.3 [a]
Ti	4990	5910	8392	3519	0.7 [a]
Zn	5730	2596	1511	3519	50 [a]
Zr	nd	761	708	198	4.2 [b]

AL—acceptable limit; [a] Hurrell et al. [83]; [b] USEPA [84].

3.4. Data Integration

The transfer factor (TF) from soil to plants is an important factor for consumption toxicity, with soil pH and OM being relevant in this process. Studied samples TF was

>1 (Figure 5), except for Pb in R4P and Zr in R1P. High TF values suggested a higher capacity of the plants to absorb contaminants [80,85]. Transfer factor was ranked RP3 > RP4 > RP2 > RP1, with sample RP3 presenting higher TF for all PTEs, with Pb being the most representative element. Lead can be absorbed from plants leaves by ash or road dust deposition, with this plant being collected in a SE wind direction over the Hulene-B landfill. Wang et al. [4] suggested that plant leaves grown in the surrounding of dumps are constantly being enriched by PTEs from ashes resulting from waste incineration. Sample RP4 Zn and Mn TF showed higher percentage rates.
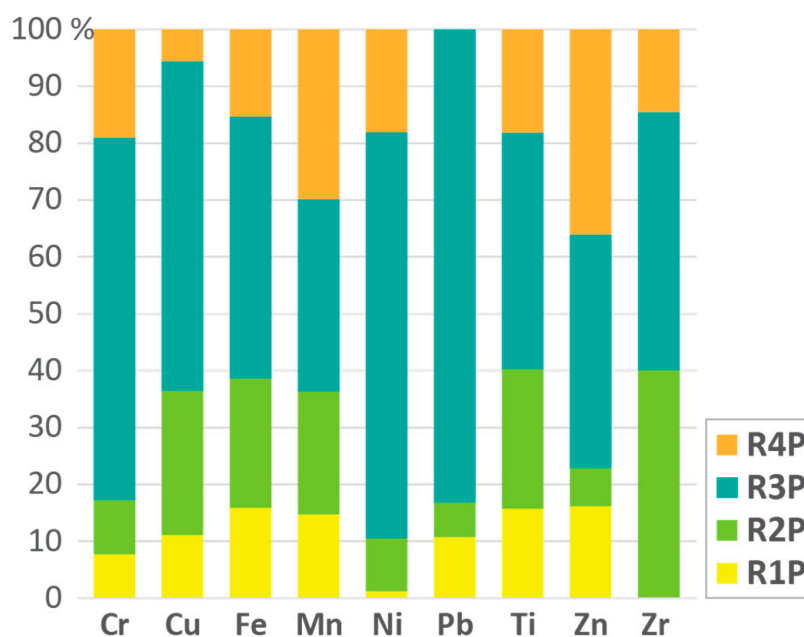
Figure 5. Transfer factor (TF) from soil to plants (relative quantification, in %).

Daily elemental intake (DIM) and hazard risk index (HRI) are presented in Table 7. Sample R1P (*Amaranthus spinosus*) DIM was ranked Fe >> Zn > Ti, with other PTEs being negligible. The HRI was high for all elements, except for Ni and Zr, being ranked Cr > Cu > Pb > Zn > Mn > Ti > Fe. Sample RP2 (*Ipomoea batatas*) DIM was >1 in Fe, Zr and Ti, while HRI > 1 was ranked Cu > Cr > Mn > Pb. Sample RP3 (*Cucurbita pepo*) DIM > 1 was ranked Fe > Cr > Ti, and HRI was ranked Cr > Cu > Pb > Ti > Mn > Ni > Zn. Sample RP4 (*Brassica oleracea L*) DIM > 1 was ranked Fe > Zn > Ti, while HRI was ranked Cr > Cu > Pb > Zn > Mn > Ti > Fe. The consumption of plants contaminated by PTEs can induce various diseases and even cancer [86]. Chromium toxicity in humans has been linked to damaged blood cells, livers, nervous systems, and kidneys [73]. Chronic Cu consumption may result in gastrointestinal irritation, diarrhea, and liver failure [87], while Fe toxicity can cause vomiting, diarrhea, and damage to the intestine and other organs [88], and Mn is linked to memory problems, hallucinations, and Parkinson's disease [89]. Nickel chronic ingestion has been associated with gastrointestinal and neurological effects including lung cancer. Ingestion of Pb can disturb almost all organs and the nervous system, in addition to causing kidney damage, brain damage, miscarriage, and death [89], and Ti can cause damage to DNA, brain [90], as well as liver and kidneys, and it can cause cancer [91], while excessive and prolonged Zn intake can lead to anemia and affect the immune system [73,90]. Zirconium, which is classified as having low toxicity [91], despite the presence and retention in relatively high amounts in biological systems, has not yet been associated with any specific metabolic function [92].

Table 7. Daily elemental intake (DIM) and hazard risk index (HRI).

Var	RP1		RP2		RP3		RP4	
	DIM	HRI	DIM	HRI	DIM	HRI	DIM	HRI
Cr	0.41	135.29	0.36	118.37	1.24	412.17	0.48	161.26
Cu	0.48	128.58	0.52	140.23	0.32	87.61	0.46	123.68
Fe	23.47	1.30	12.51	0.70	13.60	0.76	7.79	0.43
Mn	0.43	3.07	0.49	3.52	0.60	4.27	0.64	4.60
Ni	0.05	0.23	0.10	0.50	0.47	2.35	0.22	1.12
Pb	0.16	11.73	0.02	1.67	0.08	5.65	nd	nd
Ti	2.08	2.97	2.46	3.52	3.50	5.00	1.47	2.09
Zn	2.39	7.96	1.08	3.61	0.63	2.10	1.47	4.89
Zr	nd	nd	0.32	0.08	0.30	0.07	0.08	0.02

nd—not detected.

Targeted hazard quotient (THQ) and hazard index (HI$_{plant}$) are presented in Figure 6, with THQ being ranked Cr > Cu > Pb > Zn > Mn > Ni > Fe > Zr. The contribution of sample RP1 (*Amaranthus spinosus*) to induce adverse health effects in children and adults was ranked Cr > Cu > Pb > Zn > Mn > Ti > Fe, with nickel <1 and not posing potential risk for adverse health effects. Sample RP2 (*Ipomoea batatas*) Fe, Ni, and Zr content do not pose a potential health risk, with the main contributions being posed by Cu > Cr > Zn > Ti > Mn > Pb. Sample RP3 (*Brassica oleracea L*) the main contributors to potential health outcomes were ranked Cr > Cu > Pb > Ti > Mn > Ni > Zn, with Fe and Zr content representing <1. Meanwhile, sample RP4 (*Cucurbita pepo*) PTEs were ranked Cr > Cu > Zn > Mn > Ti > Ni, with Fe and Zr < 1. In all samples, the highest THQ risk index was posed to children. Similar findings were reported as a result of their lower body mass, suggesting a higher likelihood of developing cancer throughout life [41].
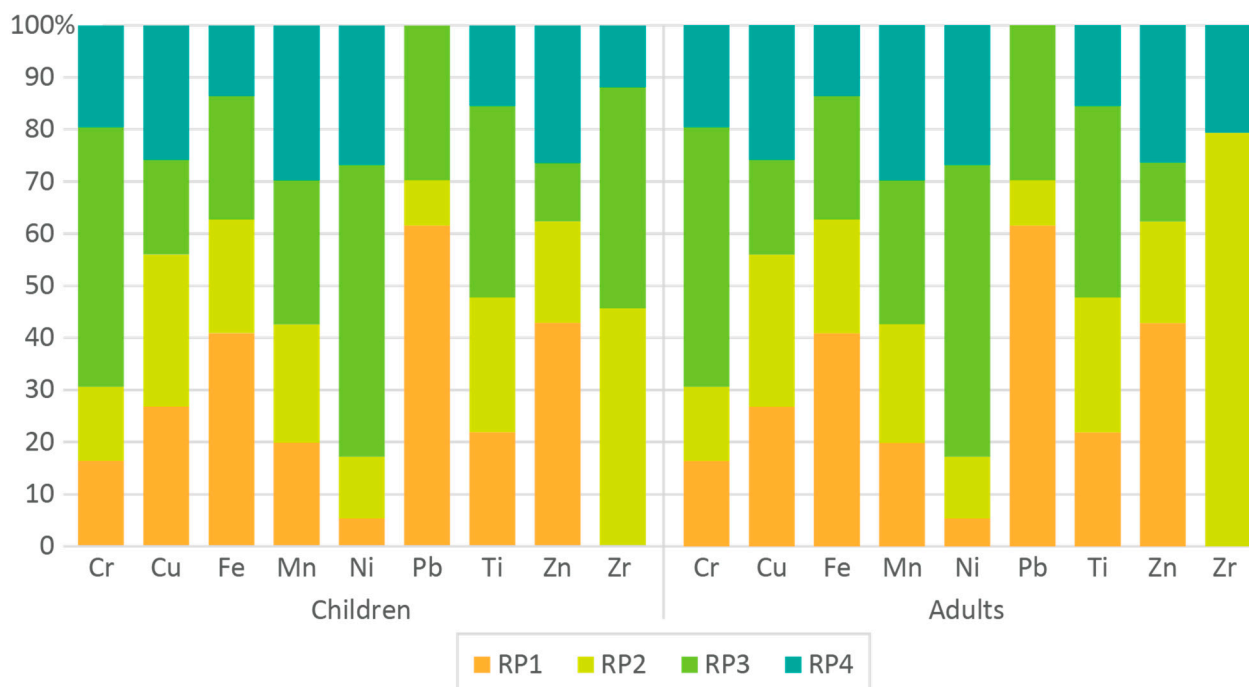
Figure 6. Targeted hazard quotient (THQ) in edible plants (relative quantification, in %).

HI$_{plant}$ was similar to THQ, being >1 in all samples and higher for children (Figure 7), being ranked RP3 (6.41×10^2 to 4.27×10^2) > RP4 (3.68×10^2 to 2.45×10^2) > RP1 (3.59×10^2 to 2.39×10^2) > RP2 (3.36×10^2–2.24×10^2). Long-term consumption of the studied plants may induce cancer (e.g., kidney, bladder, and respiratory tract), nervous system disorders, memory problems, hallucinations, cardiovascular diseases, and diabetes. In

children, this has also been associated with cognitive development problems and aggressive behavior [93,94].
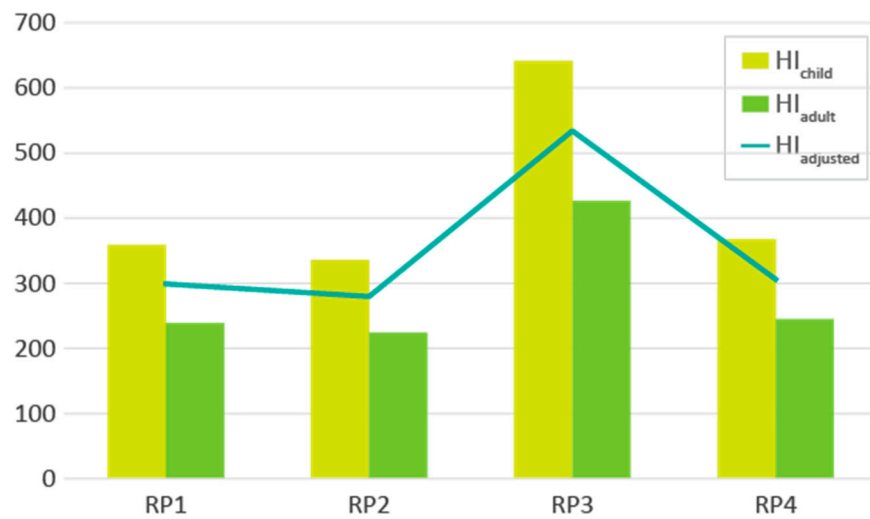

Figure 7. Hazard index in edible plants.

Well water samples systemic toxicity (non-carcinogenic hazard) presented values above 1.00×10^0 (Figure 8). The results are linked to Hg concentration, with Pb and Zn being considerably negligible. Mercury is a toxic element, being ranked the third most toxic among all PTEs [7]. It was estimated that chronic Hg consumption of about 0.00023 mg/L per day can induce adverse renal, neurological, and respiratory effects [95,96], and it can irreversibly damage kidneys, liver, and central nervous system [97]. Well waters do not present a carcinogenic risk for humans by direct consumption, with Pb showing the highest values of 1.09×10^{-7} and 6.55×10^{-7} for WN and WS, respectively, both being below the threshold of 1.00×10^{-6}. The implication of lead on human health depends on intensity, duration, and level of exposure, which can result in a range of toxic effects such as hematological, neurological, psychological, renal, and genetic mutation and reproduction are examples of the cumulative effect on the body [98]. As expected, in well waters, children had a higher health risk than adults, due to their lower body mass [41]. Lead toxicity in children can induce neurological complications, including difficulties in learning, concentration, and aggressive behavior [89]. Water ingestion is considered one of the main forms of Pb poisoning in children, accounting for about 7% [99].
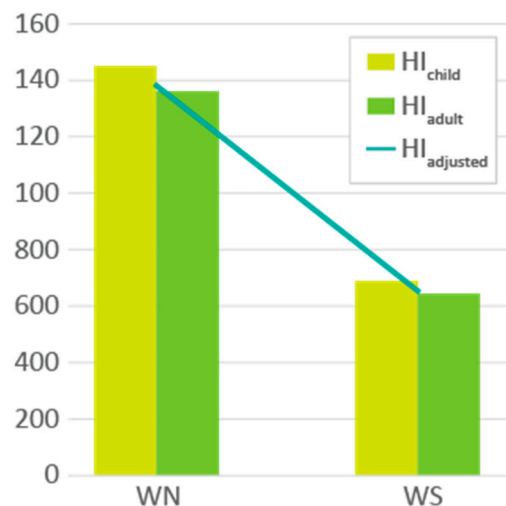

Figure 8. Systemic toxicity of well water samples.

4. Conclusions

Rhizosphere soils showed variable organic matter (OM) concentration, with moderately alkaline pH. The identified mineral phases predominance was: calcite > quartz > phyllosilicates (micas and kaolinite) > anhydrite > K feldspar > opal > gypsum, suggesting a higher ability for fixing PTEs and thus ideal conditions for adsorption and absorption of PTE in soils. The soil pollution load index (PLI) was ranked Cu >> Pb >> Zn >> Zr > Ni > Ti > Fe > Mn > Cr. Edible plants showed PTES concentration above reference dose, suggesting contamination by rhizosphere soil transfer factor and by contaminated ash deposition. Hazard index was >1 for all selected elements in all plants, except for Ni (sample RP1), Ni and Zr (sample RP2), Fe and Zr (sample R3), and Fe (sample R4), which suggests possible adverse health events. Target hazard quotient was >1 for all elements and only Zr was less than 1 in all plants. In all samples, the index was >1, and children were the ones with higher risk. Groundwater and stream waters showed a high pollution index (Pi) for Hg and Zn, with groundwater (drinking water) classified as acidic to slightly alkaline. Stream water (irrigation) was moderately alkaline, suggesting variable toxicity given PTEs concentrations above RfD.

The results suggested the need to control pollution mechanisms around the Hulene-B dump, such as leachate circulation and waste incineration ash control, the main PTEs enrichment sources of edible plants, rhizosphere soils, groundwater, and surface water. There is a need to reduce the use of well water due to high concentrations of potentially toxic elements. Farming should be relocated to other cropping areas, as part of the contamination occurs through soil transfer to plants. There is a need to protect crops from ash deposition to reduce toxicity. Future studies are needed to evaluate the levels of contamination of the waste incineration ash, and to evaluate PTEs bioaccessibility in both soil, plants, and waters.

Author Contributions: Conceptualization, C.C. and F.R.; formal analysis, B.B.; funding acquisition, F.R.; investigation, B.B., C.C. and F.R.; methodology, B.B., C.C. and F.R.; resources, F.R.; supervision, C.C. and F.R.; validation, C.C.; writing—original draft, B.B.; writing—review and editing, C.C. and F.R. All authors have read and agreed to the published version of the manuscript.

Institutional Review Board Statement: This research study does not involve animals.

Informed Consent Statement: This research study does not involve humans. This research study does not involve individual person's data in any form.

Data Availability Statement: Data used are available on the manuscript.

Conflicts of Interest: The authors declare no known competing financial interest or personal relationships that could have appeared to influence the work reported in this paper.

References

1. Dharwal, M.; Srivastava, A.K.; Sarin, V.; Gola, K. The state of solid waste management for sustainable development in India: Current state and future potential. *Mater. Today Proc.* **2021**, *60*, 802–805. [CrossRef]
2. Morita, A.K.; Ibelli-Bianco, C.; Anache, J.A.; Coutinho, J.V.; Pelinson, N.S.; Nobrega, J.; Rosalem, L.M.; Leite, C.M.; Niviadonski, L.M.; Manastella, C.; et al. Pollution threat to water and soil quality by dumpsites and non-sanitary landfills in Brazil: A review. *Waste Manag.* **2021**, *131*, 163–176. [CrossRef] [PubMed]
3. Mitra, D.; Banerji, S. Urban hydrodynamics in the planned township of New Town, West Bengal, India. *Appl. Geogr.* **2020**, *123*, 102277. [CrossRef]
4. Wang, F.; Song, K.; He, X.; Peng, Y.; Liu, D.; Liu, J. Identification of Groundwater Pollution Characteristics and Health Risk Assessment of a Landfill in a Low Permeability Area. *Int. J. Environ. Res. Public Health* **2021**, *18*, 7690. [CrossRef] [PubMed]
5. Hussein, M.; Yoneda, K.; Mohd-Zaki, Z.; Amir, A.; Othman, N. Heavy metals in leachate, impacted soils and natural soils of different landfills in Malaysia: An alarming threat. *Chemosphere* **2020**, *267*, 128874. [CrossRef] [PubMed]
6. Parvin, F.; Tareq, S.M. Impact of landfill leachate contamination on surface and groundwater of Bangladesh: A systematic review and possible public health risks assessment. *Appl. Water Sci.* **2021**, *11*, 100. [CrossRef]

7. Khattak, S.A.; Rashid, A.; Tariq, M.; Ali, L.; Gao, X.; Ayub, M.; Javed, A. Potential risk and source distribution of groundwater contamination by mercury in district Swabi, Pakistan: Application of multivariate study. *Environ. Dev. Sustain.* **2020**, *23*, 2279–2297. [CrossRef]
8. Thongyuan, S.; Khantamoon, T.; Aendo, P.; Binot, A.; Tulayakul, P. Ecological and health risk assessment, carcinogenic and non-carcinogenic effects of heavy metals contamination in the soil from municipal solid waste landfill in Central, Thailand. *Hum. Ecol. Risk Assess. Int. J.* **2020**, *27*, 876–897. [CrossRef]
9. Romero, A.; González, I.; Martín, J.M.; Vázquez, M.A.; Ortiz, P. Risk assessment of particle dispersion and trace element contamination from mine-waste dumps. *Environ. Geochem. Health* **2014**, *37*, 273–286. [CrossRef]
10. Punia, A. Role of temperature, wind, and precipitation in heavy metal contamination at copper mines: A review. *Environ. Sci. Pollut. Res.* **2020**, *28*, 4056–4072. [CrossRef]
11. Vongdala, N.; Tran, H.-D.; Xuan, T.D.; Teschke, R.; Khanh, T.D. Heavy Metal Accumulation in Water, Soil, and Plants of Municipal Solid Waste Landfill in Vientiane, Laos. *Int. J. Environ. Res. Public Health* **2018**, *16*, 22. [CrossRef]
12. Yan, X.; An, J.; Yin, Y.; Gao, C.; Wang, B.; Wei, S. Heavy metals uptake and translocation of typical wetland plants and their ecological effects on the coastal soil of a contaminated bay in Northeast China. *Sci. Total. Environ.* **2021**, *803*, 149871. [CrossRef]
13. Sharma, S.; Kaur, I.; Nagpal, A.K. Contamination of rice crop with potentially toxic elements and associated human health risks—A review. *Environ. Sci. Pollut. Res.* **2021**, *28*, 12282–12299. [CrossRef]
14. Gupta, N.; Yadav, K.K.; Kumar, V.; Krishnan, S.; Kumar, S.; Nejad, Z.D.; Khan, M.M.; Alam, J. Evaluating heavy metals contamination in soil and vegetables in the region of North India: Levels, transfer and potential human health risk analysis. *Environ. Toxicol. Pharmacol.* **2020**, *82*, 103563. [CrossRef]
15. Zhou, H.; Yang, W.-T.; Zhou, X.; Liu, L.; Gu, J.-F.; Wang, W.-L.; Zou, J.-L.; Tian, T.; Peng, P.-Q.; Liao, B.-H. Accumulation of Heavy Metals in Vegetable Species Planted in Contaminated Soils and the Health Risk Assessment. *Int. J. Environ. Res. Public Health* **2016**, *13*, 289. [CrossRef] [PubMed]
16. Halder, S.; Agüero, J.; Dolle, P.; Fernández, E.; Schmidt, C.; Yang, M. Perspectives of Urban Agriculture in Maputo and Cape Town. 2018. Available online: https://www.sle-berlin.de/files/sle/publikationen/S%20275-Maputo-Internet-Klein.pdf (accessed on 20 October 2021).
17. Bernardo, B.; Candeias, C.; Rocha, F. Application of Geophysics in geo-environmental diagnosis on the surroundings of the Hulene-B waste dump, Maputo, Mozambique. *J. Afr. Earth Sci.* **2021**, *185*, 104415. [CrossRef]
18. Serra, C. *Da Problemática Ambiental à Mudança: Rumo à um Mundo Melhor*; Editora Escolar: Maputo, Mozambique, 2012; ISBN 0A9789896700300. (In Portuguese)
19. Tvedten, I.; Candiracci, S. "Flooding our eyes with rubbish": Urban waste management in Maputo, Mozambique. *Environ. Urban.* **2018**, *30*, 631–646. [CrossRef]
20. Cendón, D.I.; Haldorsen, S.; Chen, J.; Hankin, S.; Nogueira, G.; Momade, F.; Achimo, M.; Muiuane, E.; Mugabe, J.; Stigter, T.Y. Hydrogeochemical aquifer characterization and its implication for groundwater development in the Maputo district, Mozambique. *Quat. Int.* **2019**, *547*, 113–126. [CrossRef]
21. Nogueira, G.; Stigter, T.; Zhou, Y.; Mussa, F.; Juizo, D. Understanding groundwater salinization mechanisms to secure freshwater resources in the water-scarce city of Maputo, Mozambique. *Sci. Total. Environ.* **2018**, *661*, 723–736. [CrossRef]
22. Bernardo, B.; Candeias, C.; Rocha, F. Characterization of the Dynamics of Leachate Contamination Plumes in the Surroundings of the Hulene-B Waste Dump in Maputo, Mozambique. *Environments* **2022**, *9*, 19. [CrossRef]
23. Vicente, E.M.; Jermy, C.A.; Schreiner, H.D. *Urban Geology of Maputo, Mozambique*; The Geological Society of London: London, UK, 2006; Volume 338, pp. 1–13. Available online: https://citeseerx.ist.psu.edu/viewdoc/download?doi=10.1.1.606.7220&rep=rep1&type=pdf (accessed on 20 October 2021).
24. Bernardo, B.; Candeias, C.; Rocha, F. Soil Risk Assessment in the Surrounding Area of Hulene-B Waste Dump, Maputo (Mozambique). *Geosciences* **2022**, *12*, 290. [CrossRef]
25. INE. *Boletim de Estatísticas Demográficas e Sociais, Maputo Cidade 2019*; Instituto Nacional de Estatistica: Maputo, Mozambique, 2020. Available online: https://www.ine.gov.mz/estatisticas/estatisticas-demograficas-e-indicadores-sociais/boletim-de-indicadores-demograficos-22-de-julho-de-2020.pdf/at_download/fileinportuguese (accessed on 20 October 2021).
26. Matsinhe, F.O.; Paulo, M. Estudo Etnográfico sobre os catadores de Lixo da Lixeira de Hulene (Maputo). *Cad. De África Contemp.* **2020**, *3*, 11–28.
27. dos Muchangos, L.S.; Tokai, A.; Hanashima, A. Analyzing the structure of barriers to municipal solid waste management policy planning in Maputo city, Mozambique. *Environ. Dev.* **2015**, *16*, 76–89. [CrossRef]
28. Ferrão, D.A.G. Evaluation of Removal and Disposal of Solid Waste in Maputo City, Mozambique. Master's Thesis, University of Cape Town, Cape Town, South Africa, 2006. Available online: https://open.uct.ac.za/bitstream/handle/11427/4851/thesis_sci_2006_ferrao_d_a_g.pdf?sequence=1 (accessed on 20 October 2021).
29. Palalane, J.; Segala, I.O. Urbanização e Desenvolvimento Municipal em Moçambique: Gestão de Resíduos Sólidos. 2008. Available online: https://limpezapublica.com.br/urbanizacao-e-desenvolvimento-municipal-em-mocambique-capitulo-gestao-de-residuos-solidos/ (accessed on 20 October 2021). (In Portuguese).
30. VOA (Voice of America News). Desabamento de Lixeira Deixa 17 Mortos em Maputo. 2018. Available online: https://www.voaportugues.com/a/desabamento-lixeira-17-mortos-maputo/4260624.html (accessed on 22 May 2022).

31. Muchimbane, A.B.D.A. Estudo dos Indicadores de Contaminação das Águas Subterrâneas por Sistemas de Saneamento "In Situ" Distrito Urbano 4, Cidade de Maputo-Moçambique. Ph.D. Thesis, Universidade de São Paulo, São Paulo, Brazil, 2010. [CrossRef]

32. Momade, F.J.; Ferrara, M.; Oliveira, J.T. *Notícia Explicativa da Carta Geológica 2532 Maputo (Escala 1:50000)*; Instituto Nacional de Estatistica: Maputo, Mozambique, 1996. (In Portuguese)

33. CIAT. Climate-Smart Agriculture in Mozambique. Center for Tropical Agriculture. 2017. Available online: https://climateknowledgeportal.worldbank.org/sites/default/files/2019-06/CSA-inMozambique.pdf (accessed on 14 May 2022).

34. USDA. *Rangeland Soil Quality-Organic Matter*; United States Department of Agriculture: Washington, DC, USA, 2001. Available online: https://www.ftw.nrcs.usda.gov/glti (accessed on 12 July 2022).

35. Munsell Color. *Munsell Soil Color Book*; Color Charts; Munsell Color Company Inc.: Newburgh, NY, USA, 2009.

36. USDA. *Soil Quality Indicators: pH. Managing Soils and Terrestrial Systems*; United States Department of Agriculture: Washington, DC, USA, 1998. Available online: http://soils.usda.gov (accessed on 24 July 2022).

37. USDA. *Soil Health—Electrical Conductivity*; United States Department of Agriculture: Washington, DC, USA, 2014; pp. 1–9. Available online: https://www.nrcs.usda.gov/Internet/FSE_DOCUMENTS/nrcs142p2_052803.pdf (accessed on 22 July 2022).

38. World Health Organization. *Guidelines for Drinking-Water Quality: Fourth Edition Incorporating First Addendum*; World Health Organization: Geneva, Switzerland, 2017; ISBN 978-92-4-154995-0.

39. Bhardwaj, S.; Soni, R.; Gupta, S.K.; Shukla, D.P. Mercury, arsenic, lead and cadmium in waters of the Singrauli coal mining and power plants industrial zone, Central East India. *Environ. Monit. Assess.* **2020**, *192*, 251. [CrossRef]

40. Håkanson, L. An ecological risk index for aquatic pollution control. A sedimentological approach. *Water Res.* **1980**, *14*, 975–1001. [CrossRef]

41. Candeias, C.; Ávila, P.F.; Sequeira, C.; Manuel, A.; Rocha, F. Potentially toxic elements dynamics in the soil rhizospheric-plant system in the active volcano of Fogo (Cape Verde) and interactions with human health. *Catena* **2021**, *209*, 105843. [CrossRef]

42. Zhang, H.; Zhang, F.; Song, J.; Tan, M.L.; Kung, H.-T.; Johnson, V.C. Pollutant source, ecological and human health risks assessment of heavy metals in soils from coal mining areas in Xinjiang, China. *Environ. Res.* **2021**, *202*, 111702. [CrossRef]

43. RAIS. *The Risk Assessment Information System (RAIS)*; U.S. Department of Energy's Oak Ridge Operations Office (ORO): Oak Ridge, TN, USA, 2021. Available online: https://rais.ornl.gov/ (accessed on 24 July 2022).

44. Candeias, C.; Da Silva, E.F.; Ávila, P.F.; Teixeira, J.P. Identifying Sources and Assessing Potential Risk of Exposure to Heavy Metals and Hazardous Materials in Mining Areas: The Case Study of Panasqueira Mine (Central Portugal) as an Example. *Geosciences* **2014**, *4*, 240–268. [CrossRef]

45. Pehoiu, G.; Murarescu, O.; Radulescu, C.; Dulama, I.D.; Teodorescu, S.; Stirbescu, R.M.; Bucurica, I.A.; Stanescu, S.G. Heavy metals accumulation and translocation in native plants grown on tailing dumps and human health risk. *Plant Soil* **2020**, *456*, 405–424. [CrossRef]

46. Ogunwale, T.O.; Ogar, P.A.; Kayode, G.F.; Salami, K.D.; Oyekunle, J.A.O.; Ogunfowokan, A.O.; Akindolani, O.A. Health Risk Assessment of Heavy Metal Toxicity Utilizing Eatable Vegetables from Poultry Farm Region of Osun State. *J. Environ. Pollut. Hum. Health* **2021**, *9*, 6–15. [CrossRef]

47. USEPA. Risk Assessment Guidance for Superfund. In *Volume I Human Health Evaluation Manual (Part A)*; U.S. Environmental Protection Agency: Washington, DC, USA, 1989.

48. Lee, E.; Rout, P.R.; Bae, J. The applicability of anaerobically treated domestic wastewater as a nutrient medium in hydroponic lettuce cultivation: Nitrogen toxicity and health risk assessment. *Sci. Total. Environ.* **2021**, *780*, 146482. [CrossRef]

49. Yan, C.-A.; Zhang, W.; Zhang, Z.; Liu, Y.; Deng, C.; Nie, N. Assessment of Water Quality and Identification of Polluted Risky Regions Based on Field Observations & GIS in the Honghe River Watershed, China. *PLoS ONE* **2015**, *10*, e0119130. [CrossRef]

50. Ajibare, A.O.; Ogungbile, P.O.; Ayeku, P.O. Evaluation of water pollution monitoring for heavy metal contamination: A case study of Agodi Reservoir, Oyo State, Nigeria. *Environ. Monit. Assess.* **2022**, *194*, 675. [CrossRef]

51. Adimalla, N.; Li, P.; Venkatayogi, S. Hydrogeochemical Evaluation of Groundwater Quality for Drinking and Irrigation Purposes and Integrated Interpretation with Water Quality Index Studies. *Environ. Process* **2018**, *5*, 363–383. [CrossRef]

52. Yin, Z.; Duan, R.; Li, P.; Li, W. Water quality characteristics and health risk assessment of main water supply reservoirs in Taizhou City, East China. *Hum. Ecol. Risk Assessment Int. J.* **2021**, *27*, 2142–2160. [CrossRef]

53. WHO. *Mercury in Drinking-Water, Background Document for Development of WHO Guidelines for Drinking-Water Quality*; World Health Organization: Geneva, Switzerland, 2005; WHO/SDE/WS, WHO/SDE/WSH/05.08/10. Available online: http://www.who.int/water_sanitation_health/dwq/chemicals/mercuryfinal.pdf (accessed on 1 July 2022).

54. Ahmad, W.; Alharthy, R.D.; Zubair, M.; Ahmed, M.; Hameed, A.; Rafique, S. Toxic and heavy metals contamination assessment in soil and water to evaluate human health risk. *Sci. Rep.* **2021**, *11*, 17006. [CrossRef]

55. Naveen, B.; Mahapatra, D.M.; Sitharam, T.; Sivapullaiah, P.; Ramachandra, T. Physico-chemical and biological characterization of urban municipal landfill leachate. *Environ. Pollut.* **2017**, *220*, 1–12. [CrossRef]

56. Gajaje, K.; Ultra, V.U.; David, P.W.; Rantong, G. Rhizosphere properties and heavy metal accumulation of plants growing in the fly ash dumpsite, Morupule power plant, Botswana. *Environ. Sci. Pollut. Res.* **2021**, *28*, 20637–20649. [CrossRef]

57. Škrbić, B.; Novaković, J.; Miljević, N. Mobility of heavy metals originating from bombing of industrial sites. *J. Environ. Sci. Health Part A* **2002**, *37*, 7–16. [CrossRef] [PubMed]

58. Li, H.; Sun, J.; Gui, H.; Xia, D.; Wang, Y. Physiochemical properties, heavy metal leaching characteristics and reutilization evaluations of solid ashes from municipal solid waste incinerator plants. *Waste Manag.* **2021**, *138*, 49–58. [CrossRef]

59. Chaaou, A.; Chikhaoui, M.; Naimi, M.; El Miad, A.K.; Achemrk, A.; Seif-Ennasr, M.; El Harche, S. Mapping soil salinity risk using the approach of soil salinity index and land cover: A case study from Tadla plain, Morocco. *Arab. J. Geosci.* **2022**, *15*, 722. [CrossRef]
60. Cheng, M.; Wang, H.; Fan, J.; Wang, X.; Sun, X.; Yang, L.; Zhang, S.; Xiang, Y.; Zhang, F. Crop yield and water productivity under salty water irrigation: A global meta-analysis. *Agric. Water Manag.* **2021**, *256*, 107105. [CrossRef]
61. USDA. *Soil Health Quality Indicators: Chemical Properties, Soil Electrical Conductivity*, 3rd ed.; United States Department of Agriculture: Washington, DC, USA, 2011. Available online: https://www.nrcs.usda.gov/wps/portal/nrcs/detail/soils/health/assessment/?cid=stelprdb1237387 (accessed on 12 July 2022).
62. Huang, B.; Yuan, Z.; Li, D.; Zheng, M.; Nie, X.; Liao, Y. Effects of soil particle size on the adsorption, distribution, and migration behaviors of heavy metal(loid)s in soil: A review. *Environ. Sci. Process Impacts* **2020**, *22*, 1596–1615. [CrossRef]
63. Nisari, A.; Sujatha, C. Assessment of trace metal contamination in the Kol wetland, a Ramsar site, Southwest coast of India. *Reg. Stud. Mar. Sci.* **2021**, *47*, 101953. [CrossRef]
64. Seidl, M.; Le Roux, J.; Mazerolles, R.; Bousserrhine, N. Assessment of leaching risk of trace metals, PAHs and PCBs from a brownfield located in a flooding zone. *Environ. Sci. Pollut. Res.* **2021**, *29*, 3600–3615. [CrossRef]
65. Bernardo, B.; Candeias, C.; Rocha, F. Soil properties and environmental risk assessment of soils in the surrounding area of Hulene-B waste dump, Maputo (Mozambique). *Environ. Earth Sci.* **2022**, *81*, 542. [CrossRef]
66. Alexakis, D. Multielement Contamination of Land in the Margin of Highways. *Land* **2021**, *10*, 230. [CrossRef]
67. Alexakis, D.E. Suburban areas in flames: Dispersion of potentially toxic elements from burned vegetation and buildings. Estimation of the associated ecological and human health risk. *Environ. Res.* **2020**, *183*, 109153. [CrossRef]
68. Asowata, I.T. Geophagic clay around Uteh-Uzalla near Benin: Mineral and trace elements compositions and possible health implications. *SN Appl. Sci.* **2021**, *3*, 569. [CrossRef]
69. Bai, B.; Nie, Q.; Zhang, Y.; Wang, X.; Hu, W. Cotransport of heavy metals and SiO2 particles at different temperatures by seepage. *J. Hydrol.* **2020**, *597*, 125771. [CrossRef]
70. Sharma, M.; Satyam, N.; Reddy, K.R.; Chrysochoou, M. Multiple heavy metal immobilization and strength improvement of contaminated soil using bio-mediated calcite precipitation technique. *Environ. Sci. Pollut. Res.* **2022**, *29*, 51827–51846. [CrossRef]
71. Bernardo, B.; Candeias, C.; Rocha, F. Integration of Electrical Resistivity and Modified DRASTIC Model to Assess Groundwater Vulnerability in the Surrounding Area of Hulene-B Waste Dump, Maputo, Mozambique. *Water* **2022**, *14*, 1746. [CrossRef]
72. Kazemi, Z.; Arani, M.H.; Panahande, M.; Kermani, M.; Kazemi, Z. Chemical quality assessment and health risk of heavy metals in groundwater sources around Saravan landfill, the northernmost province of Iran. *Int. J. Environ. Anal. Chem.* **2021**, 1–19. [CrossRef]
73. Cheela, V.R.S.; Goel, S.; John, M.; Dubey, B. Characterization of municipal solid waste based on seasonal variations, source and socio-economic aspects. *Waste Dispos. Sustain. Energy* **2021**, *3*, 275–288. [CrossRef]
74. Kennou, B.; El Meray, M.; Romane, A.; Arjouni, Y. Assessment of heavy metal availability (Pb, Cu, Cr, Cd, Zn) and speciation in contaminated soils and sediment of discharge by sequential extraction. *Environ. Earth Sci.* **2015**, *74*, 5849–5858. [CrossRef]
75. Githaiga, K.B.; Njuguna, S.M.; Gituru, R.W.; Yan, X. Water quality assessment, multivariate analysis and human health risks of heavy metals in eight major lakes in Kenya. *J. Environ. Manag.* **2021**, *297*, 113410. [CrossRef]
76. Yesil, H.; Molaey, R.; Calli, B.; Tugtas, A.E. Extent of bioleaching and bioavailability reduction of potentially toxic heavy metals from sewage sludge through pH-controlled fermentation. *Water Res.* **2021**, *201*, 117303. [CrossRef] [PubMed]
77. CCME. *Canadian Soil Quality Guidelines for the Protection of Environmental and Human Health-Nickel*; Canadian Council of Ministers of the Environment: Canberra, ACT, Canada, 2015. Available online: https://ccme.ca/en/res/nickel-canadian-soil-quality-guidelines-for-the-protection-of-environmental-and-human-health-en.pdf (accessed on 10 April 2022).
78. Ruengruehan, K.; Junggoth, R.; Suttibak, S.; Sirikoon, C.; Sanphoti, N. Contamination of Cadmium, Lead, Mercury and Manganese in Leachate from Open Dump, Controlled Dump and Sanitary Landfill Sites in Rural Thailand: A Case Study in Sakon Nakhon Province. *Nat. Environ. Pollut. Technol.* **2021**, *20*, 1257–1261. [CrossRef]
79. Alghamdi, A.G.; Aly, A.A.; Ibrahim, H.M. Assessing the environmental impacts of municipal solid waste landfill leachate on groundwater and soil contamination in western Saudi Arabia. *Arab. J. Geosci.* **2021**, *14*, 350. [CrossRef]
80. Islamd, S.; Idris, A.M.; Islam, A.R.M.T.; Phoungthong, K.; Ali, M.M.; Kabir, H. Geochemical variation and contamination level of potentially toxic elements in land-uses urban soils. *Int. J. Environ. Anal. Chem.* **2021**, 1–18. [CrossRef]
81. Alfaro, M.R.; Ugarte, O.M.; Lima, L.H.V.; Silva, J.R.; da Silva, F.B.V.; Lins, S.A.D.S.; Nascimento, C.W.A.D. Risk assessment of heavy metals in soils and edible parts of vegetables grown on sites contaminated by an abandoned steel plant in Havana. *Environ. Geochem. Health* **2021**, *44*, 43–56. [CrossRef]
82. Hermans, T.D.; Dougill, A.J.; Whitfield, S.; Peacock, C.L.; Eze, S.; Thierfelder, C. Combining local knowledge and soil science for integrated soil health assessments in conservation agriculture systems. *J. Environ. Manag.* **2021**, *286*, 112192. [CrossRef]
83. Hurrell, R.; Egli, I. Iron bioavailability and dietary reference values. *Am. J. Clin. Nutr.* **2010**, *91*, S1461–S1467. [CrossRef]
84. USEPA. Silver and zirconium phosphate. In *Federal Register*; U.S. Environmental Protection Agency: Washington, DC, USA, 2010; Volume 75. [CrossRef]
85. Weibel, G.; Eggenberger, U.; Schlumberger, S.; Mäder, U.K. Chemical associations and mobilization of heavy metals in fly ash from municipal solid waste incineration. *Waste Manag.* **2017**, *62*, 147–159. [CrossRef] [PubMed]

86. Balasooriya, S.; Diyabalanage, S.; Yatigammana, S.K.; Ileperuma, O.A.; Chandrajith, R. Major and trace elements in rice paddy soils in Sri Lanka with special emphasis on regions with endemic chronic kidney disease of undetermined origin. *Environ. Geochem. Health* **2021**, *44*, 1841–1855. [CrossRef] [PubMed]

87. Ashraf, I.; Ahmad, F.; Sharif, A.; Altaf, A.R.; Teng, H. Heavy metals assessment in water, soil, vegetables and their associated health risks via consumption of vegetables, District Kasur, Pakistan. *SN Appl. Sci.* **2021**, *3*, 552. [CrossRef]

88. Ali, M.U.; Liu, G.; Yousaf, B.; Abbas, Q.; Ullah, H.; Munir, M.A.M.; Fu, B. Pollution characteristics and human health risks of potentially (eco)toxic elements (PTEs) in road dust from metropolitan area of Hefei, China. *Chemosphere* **2017**, *181*, 111–121. [CrossRef] [PubMed]

89. USEPA. Manganese Compounds Hazard Summary. In *Health Effects Notebook for Hazardous Air Pollutants*; U.S. Environmental Protection Agency: Washington, DC, USA, 2016. Available online: https://www.epa.gov/sites/production/files/2016-10/documents/manganese.pdf (accessed on 1 July 2022).

90. Wani, A.L.; Ara, A.; Usmani, J.A. Lead toxicity: A review. *Interdiscip. Toxicol.* **2015**, *8*, 55–64. [CrossRef]

91. (Ans), E.P.O.F.A.A.N.S.A.T.F.; Younes, M.; Aggett, P.; Aguilar, F.; Crebelli, R.; Dusemund, B.; Filipič, M.; Frutos, M.J.; Galtier, P.; Gott, D.; et al. Evaluation of four new studies on the potential toxicity of titanium dioxide used as a food additive (E 171). *EFSA J.* **2018**, *16*, e05366. [CrossRef]

92. Price, G.A.V.; Stauber, J.L.; Holland, A.; Koppel, D.J.; Van Genderen, E.J.; Ryan, A.C.; Jolley, D.F. The Influence of pH on Zinc Lability and Toxicity to a Tropical Freshwater Microalga. *Environ. Toxicol. Chem.* **2021**, *40*, 2836–2845. [CrossRef]

93. Jones, J.V.; Piatak, N.M.; Bedinger, G.M. Zirconium and Hafnium. In *U.S. Geological Survey Professional Paper 1802*; U.S. Geological Survey: Reston, VA, USA, 2017; pp. V1–V26. [CrossRef]

94. WHO. Air Pollution. In *Compendium of WHO and Other UN Guidance on Health and Environment Chapter 2*; World Health Organization: Geneva, Switzerland, 2021; pp. 1–25. Available online: https://cdn.who.int/media/docs/default-source/who-compendium-on-health-and-environment/who_compendium_chapter2_01092021.pdf?sfvrsn=14f84896_5 (accessed on 19 April 2022).

95. WHO. *WHO Guideline for Clinical Management of Exposure to Lead Executive Summary*; World Health Organization: Geneva, Switzerland, 2021. Available online: https://www.who.int/publications/i/item/9789240036888 (accessed on 8 July 2022).

96. Ekawanti, A.; Priyambodo, S.; Kadriyan, H.; Syamsun, A.; A Lestarini, I.; Wirasaka, G.; Ardianti, A.R. Mercury pollution in water and its effect on renal function of school age children in gold mining area Sekotong West Lombok. *IOP Conf. Series Earth Environ. Sci.* **2021**, *637*, 012055. [CrossRef]

97. Fonge, B.A.; Larissa, M.T.; Egbe, A.M.; Afanga, Y.A.; Fru, N.G.; Ngole-Jeme, V.M. An assessment of heavy metal exposure risk associated with consumption of cabbage and carrot grown in a tropical Savannah region. *Sustain. Environ.* **2021**, *7*, 1909860. [CrossRef]

98. Fiala, M.; Hwang, H.-M. Influence of Highway Pavement on Metals in Road Dust: A Case Study in Houston, Texas. *Water Air Soil Pollut.* **2021**, *232*, 185. [CrossRef]

99. Obasi, P.N.; Akudinobi, B.B. Potential health risk and levels of heavy metals in water resources of lead–zinc mining communities of Abakaliki, southeast Nigeria. *Appl. Water Sci.* **2020**, *10*, 184. [CrossRef]